

## Spin-wave scattering at low temperatures in manganite films

X. J. Chen,<sup>1</sup> H.-U. Habermeier,<sup>2</sup> C. L. Zhang,<sup>1</sup> H. Zhang,<sup>2</sup> and C. C. Almasan<sup>1</sup>

<sup>1</sup>Department of Physics, Kent State University, Kent, Ohio 44242

<sup>2</sup>Max-Planck-Institut für Festkörperforschung, D-70569 Stuttgart, Germany

(Received 1 November 2002; published 3 April 2003)

The temperature  $T$  and magnetic field  $H$  dependence of the resistivity  $\rho$  has been measured for  $\text{La}_{0.8-y}\text{Sr}_{0.2}\text{MnO}_3$  ( $y=0$  and  $0.128$ ) films grown on (100)  $\text{SrTiO}_3$  substrates. The low-temperature  $\rho$  in the ferromagnetic metallic region follows well  $\rho(H,T) = \rho_0(H) + A(H)\omega_s / \sinh(\hbar\omega_s/2k_B T) + B(H)T^{7/2}$  with  $\rho_0$  being the residual resistivity. We attribute the second and third term to small-polaron and spin-wave scattering, respectively. Our analysis based on these scattering mechanisms also gives the observed difference between the metal-insulator transition temperatures of the films studied. Transport measurements in applied magnetic field further indicate that spin-wave scattering is a key transport mechanism at low temperatures.

DOI: 10.1103/PhysRevB.67.134405

PACS number(s): 75.30.-m, 72.10.-d

The observation of the colossal magnetoresistance (CMR) effect in manganite films<sup>1</sup> has produced a resurgence of interest in these materials for both fundamental physics and their possible application in recording media and magnetic switching devices. The microscopic transport mechanism in these materials has long been thought to be double exchange (DE).<sup>2-4</sup> However, it has been realized<sup>5</sup> that the effective carrier-spin interaction in the DE model is too weak to lead to a significant reduction of the electronic bandwidth, which would justify the observed several orders of magnitude increase in conductivity just below the Curie temperature  $T_C$ . Indeed, a large number of experiments have shown that the DE scenario alone cannot account for the properties of the manganites, and that CMR is not purely electronic in origin.<sup>6,7</sup>

Low-temperature charge transport measurements of manganites in the ferromagnetic metallic state are essential in clarifying the specific mechanisms responsible for the CMR effect. At low temperatures, a dominant  $T^2$  term in the resistivity has generally been observed.<sup>8-10</sup> Although the  $T^2$  behavior is consistent with electron-electron interaction,<sup>11</sup> the coefficient of the  $T^2$  term is about 60–70 times larger than the one expected for electron-electron scattering.<sup>12</sup> Moreover, a careful check of the low-temperature resistivity<sup>13,14</sup> has shown a substantial deviation from the  $T^2$ -like behavior in the very low temperature region. Other power-law temperature dependences of the resistivity have also been reported.<sup>10,14-19</sup> At present, there is no agreement on the actual scattering mechanism below the Curie temperature.

Here, we address the low-temperature scattering mechanism in manganites through resistivity measurements of  $\text{La}_{0.8-y}\text{Sr}_{0.2}\text{MnO}_3$  ( $y=0$  and  $0.128$ ) films grown on  $\text{SrTiO}_3$  substrates, measured in zero field as well as applied magnetic fields up to 14 T. Our data indicate that spin-wave scattering, which gives a  $T^{7/2}$  dependence in the low-temperature resistivity, is a dominant dissipation mechanism in the ferromagnetic state of these manganites, besides scattering of small polarons by a soft optical phonon mode. Our analysis of the resistivity data in terms of small-polaron and spin-wave scattering mechanisms, and the spin fluctuation model, also gives the observed difference in the metal-insulator transition temperature  $T_{MI}$  of the three films studied.

Thin films of  $\text{La}_{0.8}\text{Sr}_{0.2}\text{MnO}_3$  and  $\text{La}_{0.672}\text{Sr}_{0.2}\text{MnO}_3$  were grown on (100)  $\text{SrTiO}_3$  single crystal substrates by using the pulsed laser deposition technique. The substrate temperature was 750 °C, and the oxygen partial pressure in the chamber was maintained at 0.2 mbar. The growth procedure and its optimization is described elsewhere.<sup>20,21</sup> The film thickness was deduced from the deposition time normalized to calibration runs. The dc resistivity of the films was measured in zero field as well as in applied magnetic fields up to 14 T using the standard four-probe technique. The electrical current was in the film plane, perpendicular to the applied magnetic field. A constant current of 100  $\mu\text{A}$  provided by a Keithley 2400 sourcemeter was used. The magnetization  $M$  was measured in a magnetic field parallel to the film plane using a Quantum Design Superconducting Quantum Interference Device magnetometer.

Figure 1 shows zero-field resistivity data for the 200-Å lanthanum deficient  $\text{La}_{0.672}\text{Sr}_{0.2}\text{MnO}_3$  film, and for the 200- and 2000-Å  $\text{La}_{0.8}\text{Sr}_{0.2}\text{MnO}_3$  films. The 200-Å lanthanum deficient film has a  $T_{MI}$  of 364 K, which is close to that of a  $\text{La}_{0.7}\text{Sr}_{0.3}\text{MnO}_3$  single crystal.<sup>8</sup> The observed  $T_{MI}$  of 280 K for the 200-Å  $\text{La}_{0.8}\text{Sr}_{0.2}\text{MnO}_3$  is close to the values of 270 and 290 K, obtained for as-grown and annealed in  $\text{N}_2$  gas films, respectively, with same composition.<sup>22</sup> The  $T_{MI}$  of 188 K for the 2000-Å  $\text{La}_{0.8}\text{Sr}_{0.2}\text{MnO}_3$  film is lower than that for

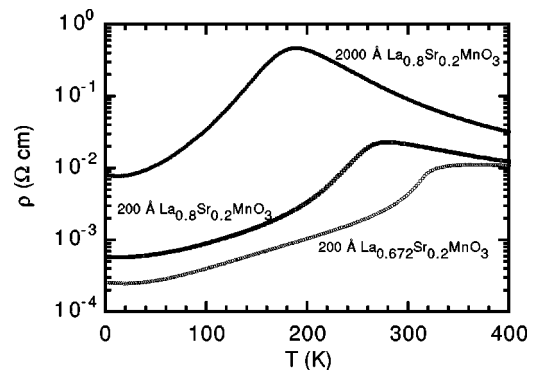


FIG. 1. Zero-field resistivity  $\rho$  as a function of temperature  $T$  of the 200-Å  $\text{La}_{0.672}\text{Sr}_{0.2}\text{MnO}_3$  film, and the 200- and 2000-Å  $\text{La}_{0.8}\text{Sr}_{0.2}\text{MnO}_3$  films, grown on (100)  $\text{SrTiO}_3$  substrates.

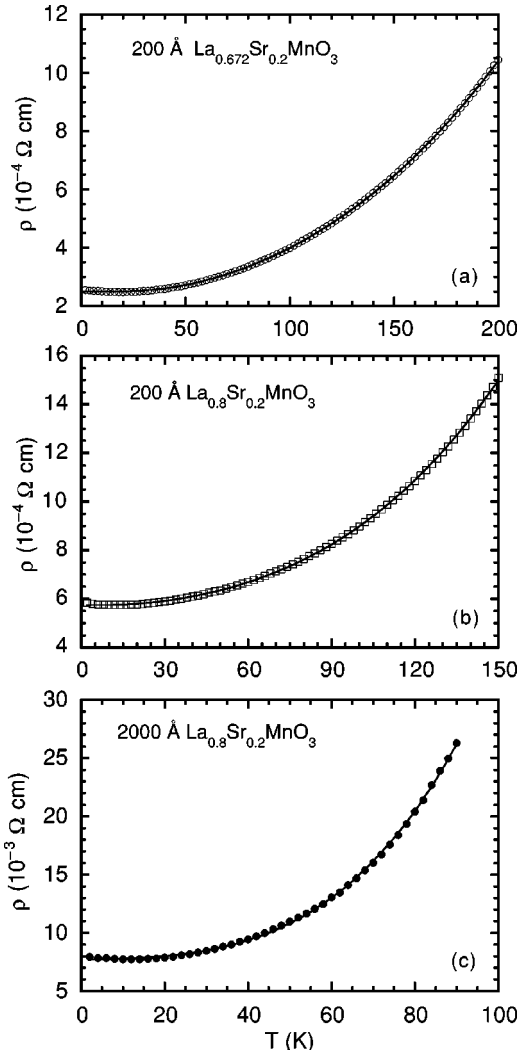


FIG. 2. Low-temperature resistivity  $\rho(T)$ , measured in zero field, for (a) the 200-Å  $\text{La}_{0.672}\text{Sr}_{0.2}\text{MnO}_3$  film, (b) the 200-Å  $\text{La}_{0.8}\text{Sr}_{0.2}\text{MnO}_3$  film, and (c) the 2000-Å  $\text{La}_{0.8}\text{Sr}_{0.2}\text{MnO}_3$  film, grown on (100)  $\text{SrTiO}_3$  substrates. The solid lines are fits of the data with Eq. (1).

single crystal specimens.<sup>8</sup> One possible explanation for this is the nonstoichiometric oxygen content in this film. In fact, a significant effect of the oxygen content on  $T_{MI}$  has been observed in  $\text{La}_{1-x}\text{Sr}_x\text{MnO}_3$  single crystals.<sup>23</sup> Thus, the composition of this low- $T_{MI}$  film is probably  $\text{La}_{0.8}\text{Sr}_{0.2}\text{MnO}_{3-\delta}$ . The  $T_C$  of each film, determined from magnetization measurements (data not shown), coincides with its  $T_{MI}$ . The residual resistivity of these films increases with decreasing

$T_{MI}$ , indicating that the films with lower  $T_{MI}$  are worse metals at low temperatures.

To elucidate the scattering mechanisms in the ferromagnetic metallic region, in Fig. 2 we plot the low-temperature behavior of the zero-field resistivity for the films studied. The resistivities of the three films can be fitted well with

$$\rho(T) = \rho_0 + \frac{A\omega_s}{\sinh^2(\hbar\omega_s/2k_B T)} + BT^{7/2}, \quad (1)$$

where  $\rho_0$ , the residual resistivity due to various temperature-independent scattering mechanisms, is taken as the resistivity at 10 K, and  $A$ ,  $\omega_s$  (average frequency of the softest optical mode), and  $B$  are fitting coefficients. The excellent fit of the data with Eq. (1) (solid curves in Fig. 2) suggests that the terms  $A\omega_s/\sinh^2(\hbar\omega_s/2k_B T)$  and  $BT^{7/2}$  capture the basic physics responsible for charge carrier scattering in this low-temperature region. The values of  $T_{MI}$ ,  $\rho_0$ , and the fitting coefficients of these films are given in Table I.

Previous reports have shown that the resistivity of  $\text{La}_{0.75}\text{Sr}_{0.25}\text{MnO}_3$  films grown on (100)  $\text{LaAlO}_3$  substrate follows well a  $\rho(T)$  dependence similar to Eq. (1) in which the third term, however, has a  $T^{9/2}$  power-law dependence, indicative of two-magnon scattering.<sup>17</sup> Nevertheless, the fit of our resistivity data with Eq. (1) for the three films studied is better over a wider temperature range than a fit in which the third term in  $\rho(T)$  is  $BT^{9/2}$ .

According to the theory of small-polaron conduction at low temperatures,<sup>24</sup> the relaxation rate  $1/\tau$  for small polarons is proportional to  $1/\sinh^2(\hbar\omega_s/2k_B T)$ .<sup>13,17</sup> Thus, the term  $A\omega_s/\sinh^2(\hbar\omega_s/2k_B T)$  in Eq. (1) is consistent with small polaron coherent motion involving relaxation due to a soft optical phonon mode.<sup>13</sup> The values of the fitting parameter  $\hbar\omega_s/2k_B$  of the  $\text{La}_{0.8-y}\text{Sr}_{0.2}\text{MnO}_3$  films are in the 15.1–71.9-K range, in agreement with values determined from low-temperature specific heat ( $\hbar\omega_s/2k_B = 48$  K) and other resistivity studies of  $\text{La}_{1-x}\text{Ca}_x\text{MnO}_3$ .<sup>13,17</sup> In addition, inelastic neutron scattering<sup>25</sup> and reflectivity<sup>26</sup> measurements support the phononic character of charge carriers for  $\text{La}_{0.8}\text{Sr}_{0.2}\text{MnO}_3$ .

We attribute the  $T^{7/2}$  dependence of the low-temperature resistivity in Eq. (1) to spin-wave scattering. The reason is the following. In the general theory of spin-wave interactions proposed by Dyson in early 1956, which gives a complete description of the thermodynamic properties of a ferromagnet at low temperatures, the mean free path  $l$  for spin-spin collisions is proportional to  $T^{-7/2}$ .<sup>27</sup> This gives a  $T^{7/2}$  temperature dependence for the resistivity since  $\rho$

TABLE I. Values of the zero field metal-insulator transition temperature  $T_{MI}$ , residual resistivity  $\rho_0$ , fitting coefficients  $A$ ,  $\hbar\omega_s/2k_B$ , and  $B$ , carrier concentration  $n$ , and activation energy  $E_A$  of  $\text{La}_{0.8-y}\text{Sr}_{0.2}\text{MnO}_3$  films grown on (100)  $\text{SrTiO}_3$  substrates. The definitions of the fitting coefficients are given in the text.

Samples	$T_{MI}$ (K)	$\rho_0$ ( $\Omega$ cm)	$A$ ( $\Omega$ cm/Hz)	$\hbar\omega_s/2k_B$ (K)	$B$ ( $\Omega$ cm/ $\text{K}^{7/2}$ )	$n$	$E_A$ (K)
200-Å $\text{La}_{0.672}\text{Sr}_{0.2}\text{MnO}_3$	364.3	$2.505 \times 10^{-4}$	$4.316 \times 10^{-18}$	71.93	$1.669 \times 10^{-12}$	$>0.2$	$\sim 1068$
200-Å $\text{La}_{0.8}\text{Sr}_{0.2}\text{MnO}_3$	280.2	$5.747 \times 10^{-4}$	$2.347 \times 10^{-18}$	26.90	$1.005 \times 10^{-11}$	$\approx 0.2$	1068
2000-Å $\text{La}_{0.8}\text{Sr}_{0.2}\text{MnO}_{3-\delta}$	188.1	$7.777 \times 10^{-3}$	$2.903 \times 10^{-17}$	15.11	$2.077 \times 10^{-9}$	$<0.2$	1546

$=m^*v_F/(ne^2l)$ , where  $m^*$  is the effective mass of the charge carriers,  $n$  is the carrier concentration, and  $v_F$  is the Fermi velocity. In fact, when the spin orientation angle between neighboring sites is small enough, the DE Hamiltonian in the low-temperature ferromagnetic state can be mapped into the Heisenberg Hamiltonian.

The temperature independent term  $\rho_0$  in Eq. (1) is usually ascribed to scattering from impurities, defects, grain boundaries, and domain walls. The values of  $\rho_0$  for the 200-Å  $\text{La}_{0.8-y}\text{Sr}_{0.2}\text{MnO}_3$  films are comparable with the value for a  $\text{La}_{0.8}\text{Sr}_{0.2}\text{MnO}_3$  single crystal,<sup>8</sup> indicating weak external scattering. In general,  $\rho_0$  is proportional to  $m^*/n\tau_0$ , where  $\tau_0$  is the zero-temperature relaxation time. Assuming that  $\tau_0$  does not change a lot among the present films, the smaller (larger) value of  $\rho_0$  for the 200-Å  $\text{La}_{0.672}\text{Sr}_{0.2}\text{MnO}_3$  film (2000-Å  $\text{La}_{0.8}\text{Sr}_{0.2}\text{MnO}_3$  film) than for the 200-Å  $\text{La}_{0.8}\text{Sr}_{0.2}\text{MnO}_3$  film indicates that  $n > 0.2$  ( $n < 0.2$ ). As discussed above,  $n < 0.2$  is probably a result of oxygen vacancies. These results for  $n$  are consistent with the defect chemistry<sup>28</sup> and are included in Table I.

Next we show that the observed difference in  $T_{MI}$  or  $T_C$  for the three films studied can be explained based on the values of the above fitting parameters. The spin fluctuation model<sup>29</sup> gives  $T_C \approx Wn(1-n)/20$ , where  $W$  is the electronic “bare” bandwidth. However, it has been shown that the huge isotope effect,<sup>6</sup> the strong sensitivity to oxygen content,<sup>30</sup> and the significant strain effect<sup>21</sup> present in these manganites can be well explained if  $W$  is replaced by an effective bandwidth  $W_{eff} \propto W \exp(-\gamma E_b/\hbar\omega)$ , where  $E_b$  is the binding energy of the polarons, which can be estimated from the activation energy  $E_A$  as  $E_b \approx 2E_A$ ,  $\omega$  is the characteristic frequency of the optical phonon mode, which can be taken as  $\omega \approx \omega_s$ , and  $\gamma$  is a positive constant. The expression of  $T_C$ , in which  $W$  is replaced by  $W_{eff}$ , shows that  $T_C$  increases as  $W$ ,  $\omega$ , and  $n$  increase (for  $n \leq 0.5$ ) and  $E_A$  decreases. Spin-wave scattering implies that the fitting coefficient  $B \propto D_s^{-7/2}$ ,<sup>14</sup> where  $D_s \propto W$  is the spin-wave stiffness coefficient.<sup>3,4</sup> Hence, an increase in  $W$  is reflected as a decrease in  $B$ . We determined  $E_A$  to be 1068 and 1546 K for the 200- and 2000-Å  $\text{La}_{0.8}\text{Sr}_{0.2}\text{MnO}_3$  films, respectively, by fitting the resistivity data in the high-temperature paramagnetic region in terms of the adiabatic small-polaron model.<sup>31</sup> We took  $E_A$  for the 200-Å  $\text{La}_{0.672}\text{Sr}_{0.2}\text{MnO}_3$  film, for which the available data in the paramagnetic region are over a narrow temperature range due to its higher  $T_{MI}$ , to be the same as  $E_A$  for the 200-Å  $\text{La}_{0.8}\text{Sr}_{0.2}\text{MnO}_3$  film.<sup>21</sup> These values of  $E_A$  are also included in Table I. As predicted above, Table I shows that, indeed, the film with larger  $\omega$  and  $n$  and smaller  $B$  and  $E_A$  has higher  $T_{MI}$ . Therefore, the present results further provide strong support for the small phonon and magnon scatterings as low-temperature dissipation mechanisms.

We now address the effect of the magnetic field on the low-temperature conduction. Figure 3 is a plot of  $\rho$  vs  $T$  data ( $T \leq 150$  K) of the 200-Å  $\text{La}_{0.8}\text{Sr}_{0.2}\text{MnO}_3$  film measured at various magnetic fields, while its inset shows  $\rho(H, T)$  over the whole measured temperature range ( $2 \leq T \leq 400$  K). Fits of the main panel data with Eq. (1), with  $A$  and  $B$  fitting parameters and  $\omega_s$  taken from zero-field fitting, give the

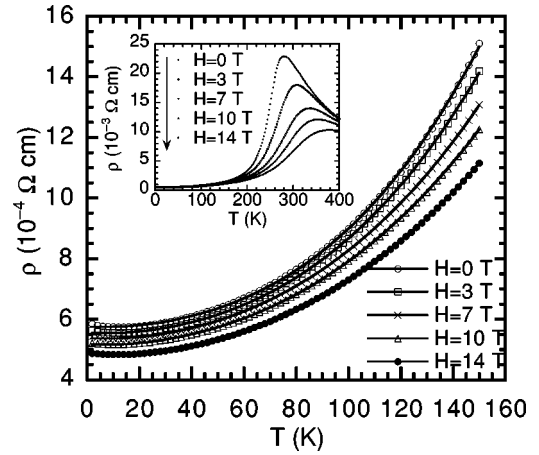


FIG. 3. Low-temperature resistivity  $\rho(T)$  of the 200-Å  $\text{La}_{0.8}\text{Sr}_{0.2}\text{MnO}_3$  film grown on a (100)  $\text{SrTiO}_3$  substrate, measured in various applied magnetic fields  $H$ . The solid lines are the fits of the data with Eq. (1). The inset shows  $\rho$  vs  $T$  for the same film over the whole measured  $T$  range at various  $H$ .

solid curves. Notice the excellent agreement between the curves and the data. Equally good fitting results were obtained for the other two films studied. This universality of charge dissipation at low temperatures with respect to thickness, composition, and magnetic field further indicates that the proposed dissipation mechanisms are intrinsic.

The above fitting has shown that  $A$  is only weak field dependent, while  $B$  has a stronger field dependence [ $B(H)$  is shown in Fig. 4]. Hence, the magnetoresistance observed in this low-temperature range is absorbed primarily in the  $T^{7/2}$  term. This is a reasonable result since this term is the spin-wave contribution to the scattering, and hence, the resistivity.

Figure 4 shows the magnetic field dependence of both  $B$  and  $T_{MI}$  of the 200-Å  $\text{La}_{0.8}\text{Sr}_{0.2}\text{MnO}_3$  film. The effect of an applied field is to open an energy gap in the magnon spectrum. As a result, the spin-wave scattering should decrease with increasing  $H$ . This is, indeed, reflected by the decrease of  $B$  with increasing  $H$ . Also note that  $T_{MI}$  increases with increasing  $H$ . This correlation between  $T_{MI}$  and  $B$  further

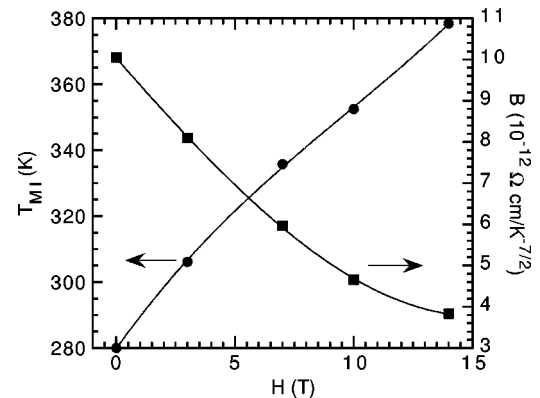


FIG. 4. Magnetic field  $H$  dependence of both the fitting parameter  $B$  (closed squares) of Eq. (1) and the metal-insulator transition temperature  $T_{MI}$  (closed circles) for the 200-Å  $\text{La}_{0.8}\text{Sr}_{0.2}\text{MnO}_3$  film grown on a (100)  $\text{SrTiO}_3$  substrate. The lines are guides to the eye.

indicates that spin-wave scattering is a key transport mechanism at low temperatures in these manganites.

In conclusion, we presented resistivity measurements in fields up to 14 T on  $\text{La}_{0.8-y}\text{Sr}_{0.2}\text{MnO}_3$  films with different compositions and/or thicknesses. Our results indicate that the dissipation mechanisms in the low-temperature ferromagnetic state are spin-wave and small-polaron scatterings. The fitting parameters obtained by analyzing the resistivity data

in terms of these dissipation mechanisms explain the observed difference in  $T_{MI}$  among the films studied. Transport measurements in applied magnetic fields indicate that spin-wave scattering is an essential dissipative mechanism at low temperatures.

This research was supported at KSU by the National Science Foundation under Grant No. DMR-0102415.

- 
- <sup>1</sup>S. Jin, T. H. Tiefel, M. McCormack, R. A. Fastnacht, R. Ramesh, and L. H. Chen, *Science* **264**, 413 (1994).
- <sup>2</sup>C. Zener, *Phys. Rev.* **82**, 403 (1951).
- <sup>3</sup>P. W. Anderson and H. Hasegawa, *Phys. Rev.* **100**, 675 (1955).
- <sup>4</sup>K. Kubo and N. Ohata, *J. Phys. Soc. Jpn.* **33**, 21 (1972).
- <sup>5</sup>A. J. Millis, P. B. Littlewood, and B. I. Shraiman, *Phys. Rev. Lett.* **74**, 5144 (1995).
- <sup>6</sup>G. M. Zhao, K. Conder, H. Keller, and K. A. Müller, *Nature (London)* **381**, 676 (1996).
- <sup>7</sup>P. C. Dai, H. Y. Hwang, J. D. Zhang, J. A. Fernandez-Baca, S.-W. Cheong, C. Kloc, Y. Tomioka, and Y. Tokura, *Phys. Rev. B* **61**, 9553 (2000).
- <sup>8</sup>A. Urushibara, Y. Moritomo, T. Arima, A. Asamitsu, G. Kido, and Y. Tokura, *Phys. Rev. B* **51**, 14 103 (1995).
- <sup>9</sup>G. J. Snyder, R. Hiskes, S. DiCarolis, M. R. Beasley, and T. H. Geballe, *Phys. Rev. B* **53**, 14 434 (1996).
- <sup>10</sup>T. Akimoto, Y. Moritomo, A. Nakamura, and N. Furukawa, *Phys. Rev. Lett.* **85**, 3914 (2000).
- <sup>11</sup>W. G. Baber, *Proc. R. Soc. London, Ser. A* **158**, 383 (1937).
- <sup>12</sup>K. Kadowaki and S. B. Woods, *Solid State Commun.* **58**, 507 (1986).
- <sup>13</sup>G.-M. Zhao, V. Smolyaninova, W. Prellier, and H. Keller, *Phys. Rev. Lett.* **84**, 6086 (2000).
- <sup>14</sup>N. Furukawa, *J. Phys. Soc. Jpn.* **69**, L1954 (2000).
- <sup>15</sup>P. Schiffer, A. P. Ramirez, W. Bao, and S.-W. Cheong, *Phys. Rev. Lett.* **75**, 3336 (1995).
- <sup>16</sup>M. Jaime, P. Lin, M. B. Salamon, and P. D. Han, *Phys. Rev. B* **58**, R5901 (1998).
- <sup>17</sup>G.-M. Zhao, D. J. Kang, W. Prellier, M. Rajeswari, H. Keller, T. Venkatesan, and R. L. Greene, *Phys. Rev. B* **63**, 060402 (2000).
- <sup>18</sup>C. L. Zhang, X. J. Chen, C. C. Almasan, J. S. Gardner, and J. L. Sarrao, *Phys. Rev. B* **65**, 134439 (2002).
- <sup>19</sup>M. J. Calderón and L. Brey, *Phys. Rev. B* **64**, 140403 (2001).
- <sup>20</sup>O. I. Lebedev, G. Van Tendeloo, S. Amelinckx, B. Leibold, and H.-U. Habermeier, *Phys. Rev. B* **58**, 8065 (1998).
- <sup>21</sup>X. J. Chen, S. Soltan, H. Zhang, and H.-U. Habermeier, *Phys. Rev. B* **65**, 174402 (2002).
- <sup>22</sup>H. L. Ju, C. Kwon, Q. Li, R. L. Greene, and T. Venkatesan, *Appl. Phys. Lett.* **65**, 2108 (1994).
- <sup>23</sup>R. Shiozaki, K. Takenaka, Y. Sawaki, and S. Sugai, *Phys. Rev. B* **63**, 184419 (2001).
- <sup>24</sup>I. G. Lang and Yu. A. Firsov, *Zh. Éksp. Teor. Fiz.* **43**, 1843 (1962) [*Sov. Phys. JETP* **16**, 1301 (1963)].
- <sup>25</sup>W. Reichardt and M. Braden, *Physica B* **263-264**, 416 (1999).
- <sup>26</sup>J. Coulon, A. Hassini, M. Gervais, A. Douy, C. Champeaux, J. Lecomte, L. Ammor, A. Catherinot, J.-B. Quoirin, and F. Gervais, *Mater. Sci. Eng., B* **83**, 227 (2001).
- <sup>27</sup>F. J. Dyson, *Phys. Rev.* **102**, 1217 (1956).
- <sup>28</sup>J. A. M. van Roosmalen and E. H. P. Cordfunke, *J. Solid State Chem.* **110**, 109 (1994).
- <sup>29</sup>C. M. Varma, *Phys. Rev. B* **54**, 7328 (1996).
- <sup>30</sup>J. M. De Teresa, K. Dörr, K. H. Müller, L. Schultz, and R. I. Chakalova, *Phys. Rev. B* **58**, R5928 (1998).
- <sup>31</sup>D. Emin and T. Holstein, *Ann. Phys. (N.Y.)* **53**, 439 (1969).